

000 001 002 003 004 005 006 007 008 009 010 011 012 013 014 015 016 017 018 019 020 021 022 023 024 025 026 027 028 029 030 031 032 033 034 035 036 037 038 039 040 041 042 043 044 045 046 047 048 049 050 051 052 053 MULTI-SCALE SPATIAL-TEMPORAL HYPERGRAPH NETWORK WITH LEAD-LAG STRUCTURES FOR STOCK TIME SERIES FORECASTING

Anonymous authors

Paper under double-blind review

ABSTRACT

Time series forecasting occurs in a range of financial applications providing essential decision-making support to investors, regulatory institutions, and analysts. Unlike multivariate time series from other domains, stock time series exhibit industry correlation. Exploiting this kind of correlation can improve forecasting accuracy. However, existing methods based on hypergraphs can only capture industry correlation relatively superficially. These methods face two key limitations: they do not fully consider inter-industry lead-lag interactions, and they do not model multi-scale information within and among industries. This study proposes the **Hermes** framework for stock time series forecasting that aims to improve the exploitation of industry correlation by eliminating these limitations. The framework integrates moving aggregation and multi-scale fusion modules in a hypergraph network. Specifically, to more flexibly capture the lead-lag relationships among industries, Hermes proposes a hyperedge-based moving aggregation module. This module incorporates a sliding window and utilizes dynamic temporal aggregation operations to consider lead-lag dependencies among industries. Additionally, to effectively model multi-scale information, Hermes employs cross-scale, edge-to-edge message passing to integrate information from different scales while maintaining the consistency of each scale. Experimental results on multiple real-world stock datasets show that Hermes outperforms existing state-of-the-art methods in both efficiency and accuracy. All datasets and code are available at <https://anonymous.4open.science/r/Hermes-E150>.

1 INTRODUCTION

Stock time series are typically composed of data from multiple stocks, each of which includes multiple key indicators such as stock opening prices, closing prices, etc. (Fan & Shen, 2024; Li et al., 2024). Stock time series forecasting (STSF) is important in financial applications, providing crucial decision-making support for investors, regulatory institutions, and analysts, helping them make data-driven decisions in complex and ever-changing market environments (Rather et al., 2017; Faloutsos et al., 2018; Jacob & Shasha, 1999; Zhang et al., 2014; Zheng et al., 2023).

Most existing studies treat stocks in stock time series independently, thus disregarding the interconnected nature of market dynamics and contradicting the intrinsic interdependencies observed in real-world financial systems (Diebold & Yilmaz, 2014). In reality, stocks are often interrelated, and there are rich signals in the relationships between them (Nobi et al., 2014). For example, with the breakthroughs of Artificial Intelligence technology, companies like Apple, Microsoft, and Alphabet that actively invest and innovate in this domain are expected to lead in the market due to their technological advantages. It is one of the important factors for their stock prices to show a steady upward trend in the overall stock market¹—see Figure 1a. At the same time, the soaring power demand, driven by electrification, decarbonization, and the advent of artificial intelligence, led to a concurrent rise in the stock prices of companies in the energy sector²—see Figure 1a. Such industry correlations have gradually attracted more attention. Especially within the same industry, different

¹ www.morningstar.co.uk/news/258865/tech-and-communication-stocks-drove-us-market-gains-in-2024.aspx

² <https://finance.yahoo.com/news/american-electric-power-aep-among-121752028.html?>

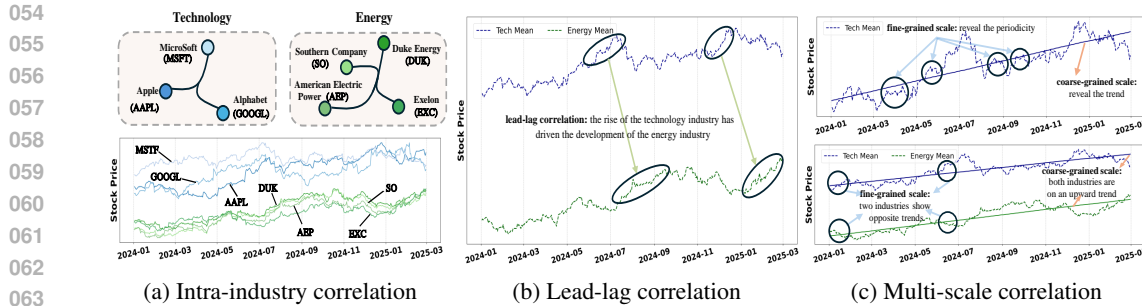


Figure 1: (a): Intra-industry correlation. Relations between stocks within an industry (hyperedge) can be represented by a hypergraph. (b): Lead-lag correlation. (c): Multi-scale correlation.

stocks often exhibit correlations, reflecting the common economic environment, market fluctuations, policy changes, and other factors that impact the stocks.

Hypergraphs can connect multiple graph nodes (representing, e.g., stocks) through hyperedges. By connecting stocks within the same industry by hyperedges to construct a hypergraph network, it is possible to capture more comprehensively the interrelationships and dynamics among stocks within an industry. However, existing hypergraph-based STSF methods that consider industry correlations still have the following challenges.

Challenge 1: Current methods fail to fully consider inter-industry lead-lag interactions. In financial markets, there are causal relationships and time dependencies among industries, and these relationships are highly diverse and complex. As shown in Figure 1b, the technology industry has flourished with breakthroughs in key technologies and market innovations, achieving significant progress. Technological innovations from technology companies have injected new vitality into the development of renewable energy, and energy companies have leveraged technologies such as big data, AI, and the Internet of Things to enhance the efficiency of energy production and management², thereby driving up stock prices (Abid et al., 2025; Olanrewaju et al., 2024; Rafiee et al., 2025). Therefore, in the modeling process, it is important to capture lead-lag correlations among industries more accurately, so as to better reflect the dynamic interactions and dependencies in financial markets, ultimately improving the accuracy and practicality of the forecasts.

Challenge 2: Current methods do not model multi-scale information within and among industries. Stock time series inherently possess multi-scale characteristics, and markets exhibit different features and patterns at different time scales. For example, in Figure 1c, we can observe a clear overall trend at a coarse-grained scale, and a cyclical pattern at a fine-grained scale. Moreover, two different industries, may exhibit correlations at a coarse-grained scale. However, delving deeper into a fine-grained analysis might find that two industries show opposite trends. Single-scale analysis methods cannot fully capture such characteristics, so there is a pressing need to adopt multi-scale analysis to reveal the dynamic changes in financial markets across different time scales, thereby providing richer and more accurate information for stock time series forecasting.

In this study, we address the two challenges by proposing a general stock time series forecasting framework, **Hermes**, which integrates *hyperedge-based moving aggregation* and *hyperedge-based multi-scale fusion* modules into a spatial-temporal hypergraph network. These integrations enhance the precision and stability of stock forecasting. First, to more flexibly model lead-lag relationships among industries, we integrate a *hyperedge-based moving aggregation module* into the hypergraph network. This module incorporates a sliding window and utilizes dynamic temporal aggregation operations to consider lead-lag dependencies among industries. This approach aims to capture a market's complex structure more precisely. Second, to address the issue that existing methods fail to effectively model multi-scale information, we decompose raw data at multiple scales and integrate a *multi-scale fusion module* into the hypergraph network. This module employs cross-scale, edge-to-edge message passing to integrate information from different scales while preserving the consistency of each scale, thereby boosting both the accuracy and stability of forecasts. Experimental results on multiple real-world stock datasets show that Hermes outperforms existing state-of-the-art methods in both efficiency and accuracy. Our contributions are summarized as follows.

- 108 • To solve the STSF problem, we propose a general spatial-temporal hypergraph network frame-
109 work, **Hermes**, which learns more accurate and adaptive forecasting models by considering both
110 lead-lag and multi-scale industry correlations.
- 111
- 112 • We design a hyperedge-based multi-scale fusion module. This module utilizes a cross-scale,
113 egde-to-edge message-passing to integrate information from different scales while maintaining
114 the consistency of each scale.
- 115
- 116 • We propose a hyperedge-based moving aggregation module that introduces a sliding window
117 and utilizes dynamic temporal aggregation operations to consider lead-lag dependencies among
118 industries.
- 119
- 120 • We report on extensive experiments on public stock datasets, finding that Hermes is capable of
121 outperforming state-of-the-art baselines.

123 2 RELATED WORK

124 2.1 DEEP LEARNING STOCK TIME SERIES FORECASTING

125 With the rise of deep learning, notable progress has occurred in stock forecasting. This is mainly
126 because deep neural networks can model complex nonlinear patterns. Some studies use recurrent
127 neural networks (RNNs) (Nelson et al., 2017; Qin et al., 2017; Akita et al., 2016; Rahman et al.,
128 2019) to capture the historical development in individual stock prices and predict their short-term
129 trends. In addition, due to the significant progress of Multi-Layer Perceptrons (MLPs) architecture
130 in the general time series field (Zeng et al., 2023; Lin et al., 2025; 2024). Increasingly may proposals
131 target stock forecasting performance by improving the MLPs architecture. For example, a series of
132 studies (Fan & Shen, 2024; Lazcano et al., 2024; Tashakkori et al., 2024) enhance the learning abil-
133 ity of simple MLPs structures by utilizing the MLP-Mixer backbone, thereby improving forecasting
134 accuracy. Next, the Transformer model has become increasingly popular due to the ability of its
135 self-attention mechanism to capture long-term dependencies. For example, Master (Li et al., 2024)
136 proposes a novel stock transformer for stock price forecasting to effectively capture stock correla-
137 tion. While these deep learning methods have advanced stock forecasting, the complexity of stock
138 data and the need to account for intricate relationships among stocks have led researchers to explore
139 new methods based on hypergraphs.

140 2.2 HYPERGRAPH-BASED STOCK TIME SERIES FORECASTING

141 Traditional graphs have limitations when it comes to modeling higher-order multivariate relation-
142 ships, as they can only represent relations between pairs of nodes. To address this issue, Hypergraph
143 Neural Networks (HGNNS) (Feng et al., 2019c) were introduced. Hypergraphs extend the concept
144 of simple graphs to enable the capture of relationships among multiple stocks (Chen et al., 2020).
145 Hypergraphs have gained increasing attention and application across various fields. Hyperedge in
146 a hypergraph represents a set of vertices, making them suitable for modeling non-pairwise rela-
147 tionships (Luo et al., 2014; Sawhney et al., 2020; Huynh et al., 2023). For example, HGAM (Li
148 et al., 2022) is a hypergraph-based reinforcement learning method for stock portfolio selection.
149 THGNN (Xiang et al., 2022) is a temporal and heterogeneous graph neural network model that
150 aims to learn dynamic relationships by using two-stage attention mechanisms. STHAN-SR (Sawh-
151 ney et al., 2021) enhances corporate relevance based on Wiki data and uses hypergraph convolution
152 to propagate information from higher-order neighbors. ESTIMATE (Huynh et al., 2023), employs
153 hypergraphs to capture non-pairwise correlations, utilizing temporal generative filters to identify
154 individual patterns for each stock. Unlike the above methods, we propose a new hypergraph-based
155 stock time series forecasting model that specifically takes into account the multi-scale nature of stock
156 data, enabling it to capture the complexity of market dynamics more comprehensively. Furthermore,
157 our approach places particular emphasis on the lead-lag relationships between financial industries,
158 where the changes in one industry may precede or lag behind those in another. By capturing these
159 key relationships more fully, we aim to improve forecasting accuracy.

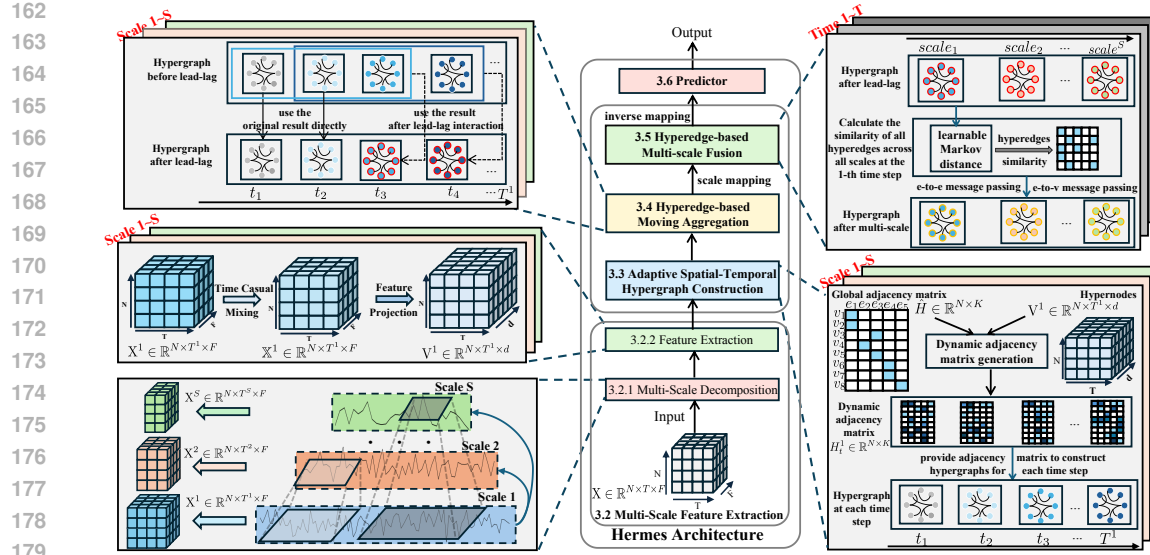


Figure 2: The architecture of Hermes.

3 METHODOLOGY

In financial markets, a stock time series $\mathbf{X} = \{X_1, \dots, X_N\}$ records the historical data of N stocks, where $X_i \in \mathbb{R}^{T \times F}$ is data of one stock with a lookback window of T time steps and with F technical indicators at each time step. In stock time series, the indicators may include opening price, closing price, highest price, lowest price, and trading volume. Following existing studies (Huynh et al., 2023; Fan & Shen, 2024), we input a stock time series with multiple indicators, denoted as $\mathbf{X} \in \mathbb{R}^{N \times T \times F}$, and aim to predict the closing price p_i^t at time step t . We define the 1-day return ratio as $r_i^t = \frac{p_i^t - p_i^{t-1}}{p_i^{t-1}}$. With θ representing the model parameters, the process can be expressed as follows.

$$\mathbf{X} \in \mathbb{R}^{N \times T \times F} \xrightarrow{\theta} p \in \mathbb{R}^{N \times 1} \rightarrow r \in \mathbb{R}^{N \times 1} \quad (1)$$

3.1 FRAMEWORK OVERVIEW

In this section, we introduce the framework of our proposed spatiotemporal hypergraph neural network that considers multiple time scales and models the lead-lag relationships between industries. Our framework takes historical financial sequences as input, first samples the time series into several sequences of different granularities according to different time scales, and maps the feature dimension to the hidden dimension to consider the high-dimensional correlations between time series segments under different scales. Subsequently, we consider constructing relationships between agents at each scale, specifically considering constructing hyperedges for agents in the same industry, and modeling the lead-lag relationships between industries in the corresponding hypergraphs. Then, we model the interactions between different scales, construct hyperedges for industries of different scales, and adaptively learn the correlations between them under the corresponding multi-scale hypergraph, thereby playing a role in fusing scales. Finally, we predict the corresponding indicators for each agent for the next day through a prediction head based on a multilayer perceptron.

3.2 MULTI-SCALE FEATURE EXTRACTION

Multi-Scale Decomposition. Time series of different scales exhibit different characteristics, among which fine scales primarily describe detailed patterns and contain more periodic information, while coarse scales highlight macro changes and cover the overall trend changes. This multi-scale perspective can essentially unravel the complex variations within multiple components, thereby facilitating time variation modeling. It is worth noting that, especially for prediction tasks, due to their different dominant time patterns, multi-scale time series show different predictive capabilities.

216 Specifically, for the financial input time series $\mathbf{X} \in \mathbb{R}^{N \times T \times F}$, which denotes the records of F
 217 key indicators for N market agents of T timestamps in the past. To decouple the intricate multi-
 218 resolution information, we use convolutional layers of different sizes to adaptively down-sample the
 219 time series into sequences of different scales:

$$220 \quad \mathbf{X}^i = \text{1D-Conv}^i(\mathbf{X}), \quad (2)$$

222 where $\mathbf{X}^i \in \mathbb{R}^{N \times T^i \times F}$ denotes the i -th scale of financial time series, T^i is the down-sampled length.
 223 We then obtain the multi-scale time series sequences $\{\mathbf{X}^1, \mathbf{X}^2, \dots, \mathbf{X}^S\}$ of S kinds of scales through
 224 S convolutional layers with different kernel sizes and stride lengths.
 225

226 **Feature Extraction.** Subsequently, for time series of different scales, we enhance their representa-
 227 tions at two aspects. First, we adopt the Causal-Mixing technique to process the temporal dimen-
 228 sional. The Causal-Mixing technique ensures causal relationships rather than full connectivity, and
 229 ensure that time series points can only see previous points. It consists of a group of MLP layers:

$$230 \quad \text{Causal-Mixing}^i = \{\text{MLP}^{i,1}, \text{MLP}^{i,2}, \dots, \text{MLP}^{i,T^i}\}, \quad \text{MLP}^{i,j} = \mathbb{R}^j \rightarrow \mathbb{R} \quad (3)$$

$$231 \quad \mathbb{X}^i = \text{Causal-Mixing}^i(\mathbf{X}^i), \quad (4)$$

233 the Causal-Mixing is applied along the temporal dimensional, which maps $X_{1:j}^i$ through $\text{MLP}^{i,j}$ to
 234 \mathbb{X}_j^i . The new representation $\mathbb{X} \in \mathbb{R}^{N \times T^i \times F}$ keeps the original shape.
 235

236 Then their feature dimensions are mapped into the high-dimension hidden spaces to enrich their
 237 representation capabilities, facilitating the extraction of more complex hidden relationships:

$$238 \quad \mathcal{X}^i = \mathbb{X}^i \cdot \mathbf{W}^i, \quad (5)$$

240 where $\mathcal{X}^i \in \mathbb{R}^{N \times T^i \times d}$, d is the dimension of the latent space. $\mathbf{W}^i \in \mathbb{R}^{F \times d}$, constructing a linear
 241 projection to enhance representational capability.
 242

243 3.3 ADAPTIVE SPATIAL-TEMPORAL HYPERGRAPH CONSTRUCTION

245 For the representation $\mathcal{X}^i \in \mathbb{R}^{N \times T^i \times d}$ of i -th scale, the hypergraph of i -th scale \mathcal{X}^i can be con-
 246 structed through a global-shared matrix $H \in \mathbb{R}^{N \times K}$, where N represents the number of stocks, K
 247 represents the number of industries, and $H_{l,m} = 1$ denotes that the l -th stock belongs to the m -th
 248 industry. The i -th Spatial-Temporal hypergraph \mathcal{G}^i is formulated as:

$$249 \quad \mathcal{G}^i = (H, \mathcal{X}^i, E^i), \quad (6)$$

251 where \mathcal{X}^i is the representation of i -the scales and works as the nodes of the \mathcal{G}^i , $E^i \in \mathbb{R}^{K \times T^i \times d}$ is
 252 the hyperedge constructed through the stock-industry relationship matrix H :
 253

$$254 \quad \text{scores}^i = \text{Linear}^i(\mathcal{X}^i) \in \mathbb{R}^{N \times 1}, \quad \text{Linear}^i = \mathbb{R}^{T^i \times d} \rightarrow \mathbb{R}, \quad (7)$$

$$255 \quad H^i = H \odot \text{scores}^i + (1 - H) \odot (-\infty), \quad \mathcal{H}^i = \text{SoftMax}(H^i, \text{dim} = 0), \quad E^i = (\mathcal{H}^i)^T \cdot \mathcal{X}^i, \quad (8)$$

257 where the matrix H is first processed with a learnable renovation to adapt to the current representa-
 258 tion \mathcal{X}^i . H^i is the intermediate result obtained through endowing the $H_{l,m} = 1$ parts with learnable
 259 scores i and $H_{l,m} = 0$ parts with $-\infty$ to ensure zeros in the SoftMax step. Then the $\mathcal{H}^i \in \mathbb{R}^{N \times K}$
 260 with Continuous Weights is obtained, and the hyperedges $E^i \in \mathbb{R}^{K \times T^i \times d}$ of industries are gener-
 261 ated through information integration from all the related agents. We obtain all the Spatial-Temporal
 262 hypergraphs $\{\mathcal{G}^1, \mathcal{G}^2, \dots, \mathcal{G}^S\}$ for each scale as above mentioned.
 263

264 3.4 HYPEREDGE-BASED MOVING AGGREGATION

265 After delineating different time series scales with Spatial-Temporal hypergraphs $\{\mathcal{G}^1, \mathcal{G}^2, \dots, \mathcal{G}^S\}$,
 266 we further consider the lead-lag relationships between industries under each scale, to analyze the
 267 complex correlations in financial markets—see Figure 3 in Appendix B.4.
 268

269 We construct a message passing mechanism on the hyperedges to capture the lead-lag relationships
 between industries. First, we employ a fixed-size sliding window as the range for examining the

270 lead-lag relationships. For each hyperedge, through the sliding window, we can delineate different
 271 patches, which serve as the smallest units for constructing the lead-lag relationships:
 272

$$\mathcal{P}^i = \text{SlidingWindow}(E^i, \text{size} = k^i, \text{stride} = 1), \quad (9)$$

274 where $\mathcal{P}^i \in \mathbb{R}^{K \times (T^i - k^i + 1) \times k^i \times d}$ denotes the patches of E^i , containing local information with the
 275 size of k^i . From the perspective of causality, considering the relationship between the first few
 276 points and the last point within the window, we can construct the relationship matrix of the leading
 277 part and the lagging part. We then mine the lead-lag relationships inside each patch by considering
 278 the correlations between \mathcal{P}_{before}^i and \mathcal{P}_{last}^i :

$$\mathcal{P}_{before}^i = \text{Reshape}(\mathcal{P})^i \in \mathbb{R}^{[K \times (T^i - k^i + 1)] \times k^i \times d}, \quad (10)$$

$$\mathcal{P}_{last}^i = \text{Reshape}(\mathcal{P})_{-1}^i \in \mathbb{R}^{(K \times 1) \times k^i \times d}, \quad (11)$$

283 Subsequently, by using the message passing method to propagate through the leading part, we obtain
 284 the feature fusion among hyperedges:

$$\tilde{A}^i = \mathcal{P}_{before}^i \otimes \mathcal{P}_{last}^i \in \mathbb{R}^{[K \times (T^i - k^i + 1)] \times K \times k^i}, \quad (12)$$

$$A^i = \text{SoftMax}(\tilde{A}^i, \text{dim} = 2), \quad \tilde{E}^i = A^i \otimes \mathcal{P}_{before}^i \in \mathbb{R}^{K \times k^i \times d}, \quad (13)$$

$$\hat{E}^i = \text{MLP}^i(\tilde{E}^i) + E^i, \quad \text{MLP}^i := \mathbb{R}^{k^i} \rightarrow \mathbb{R}^{T^i}, \quad \mathcal{V}^{e^i} = \hat{E}^i \otimes \mathcal{H} \in \mathbb{R}^{N \times T^i \times d}, \quad (14)$$

290 where \tilde{A}^i considers the correlations among the leading parts and lagging parts, A^i probabilityizes
 291 \tilde{A}^i to control weightsuming, $\hat{E}^i \in \mathbb{R}^{K \times T^i \times d}$ denotes the embedding of hyperedges integrated with
 292 lead-lag relationships among different industries. \mathcal{V}^{e^i} is the updated nodes of i -th scale integrated
 293 with the lead-lag information extracted on hyperedges—see Figure 4 in Appendix B.4.

294 This is the method of considering the leading and lagging relationships between industries under
 295 each scale using Spatial-Temporal hypergraphs. After performing the above operation for each
 296 scale, we obtain a multi-scale representation of hyperedges $\{\hat{E}^1, \hat{E}^2, \dots, \hat{E}^S\}$. Subsequently, fu-
 297 sion between scales will be carried out to integrate information of different granularities.
 298

3.5 HYPEREDGE-BASED MULTI-SCALE FUSION

301 For multi-scale representation of hyperedges $\{\hat{E}^1, \hat{E}^2, \dots, \hat{E}^S\}$ which contains the industry in-
 302 formation, we further extract the potential correlations among different scales to reveal the latent
 303 interactions among different industries. First, we up-sample different scales back to the original
 304 length to ensure uniform representation size:

$$\hat{\mathcal{E}}^i = \text{Linear}^i(\hat{E}^i) \in \mathbb{R}^{K \times T \times d}, \quad \text{Linear}^i = \mathbb{R}^{T^i} \rightarrow \mathbb{R}^T, \quad (15)$$

$$\hat{\mathcal{E}} = \{\hat{\mathcal{E}}^1, \hat{\mathcal{E}}^2, \dots, \hat{\mathcal{E}}^S\} \in \mathbb{R}^{S \times K \times T \times d} \quad (16)$$

308 Then, we construct adaptive adjacency matrices for these hyperedges of different scales to measure
 309 the correlations between different industries at various information granularities. We employ metric
 310 learning for this task and use a learnable Mahalanobis distance to automatically build relationships
 311 between different industries in the hidden space:

$$\tilde{\mathcal{E}} = \text{Flatten}(\hat{\mathcal{E}}) \in \mathbb{R}^{(S \times K) \times T \times d}, \quad D_{ij} = (\tilde{\mathcal{E}}_i - \tilde{\mathcal{E}}_j)^T \otimes Q \otimes (\tilde{\mathcal{E}}_i - \tilde{\mathcal{E}}_j), \quad (17)$$

$$C_{ij} = \begin{cases} \frac{1}{D_{ij}} & \text{if } i \neq j \\ 0 & \text{if } i = j \end{cases}, \quad B = \text{SoftMax}(C, \text{dim} = 0) \quad (18)$$

317 where $D, C, B \in \mathbb{R}^{(S \times K) \times (S \times K) \times T \times d}$. $Q \in \mathbb{R}^{d \times d}$ is a learnable semi-positive definite matrix,
 318 and can be practically constructed by $Q = L^T \cdot L$. Subsequently, we construct interactions be-
 319 tween hyperedges at different scales using message passing and further update the representation of
 320 hyperedges.

$$\tilde{B} = \mathcal{D}^{-1} \otimes B \otimes \mathcal{D}, \quad \mathcal{E}' = \tilde{B} \otimes \tilde{\mathcal{E}} \otimes W^e, \quad (19)$$

321 where $\mathcal{D} \in \mathbb{R}^{(S \times K) \times T \times d}$ is the degree matrix, $W^e \in \mathbb{R}^{d \times d}$ is the learnable parameters in the
 322 graph message passing mechanism. After integrating the lead-lag relationships between industries

324 on the hyperedges and fusing the hidden relationships between different scales, the representation
 325 of the hyperedges \mathcal{E}' is adaptively updated. We then continue to complete the message passing from
 326 hyperedges to nodes—see Figure 4 in Appendix B.4, thereby feeding back the complex correlations
 327 within the industry to specific agents and completing the update of the representation of agent nodes:

$$328 \quad \mathcal{V} = \mathcal{E}' \otimes \mathcal{H} \in \mathbb{R}^{(S \times N) \times T \times d} \quad (20)$$

330 3.6 PREDICTOR

332 After completing the complex representation extraction using a hypergraph-based structure, we em-
 333 ploy an MLP-based predictor and incorporate residual connection modules to forecast financial in-
 334 dicators across each scale s .

$$335 \quad \hat{\mathcal{X}}^s = \text{MLP}_{s,1}(\mathcal{X}^s) \in \mathbb{R}^{N \times 1}, \quad \tilde{\mathcal{V}}^s = \text{MLP}_{s,2}(\mathcal{V}^s) \in \mathbb{R}^{N \times 1}, \quad (21)$$

$$337 \quad \hat{Y}^s = \hat{\mathcal{X}}^s + \tilde{\mathcal{V}}^s, \quad \hat{Y} = \sum_{s=1}^S \hat{Y}^s, \quad (22)$$

339 where $X^s \in \mathbb{R}^{(N \times T^s \times d)}$ represents the initial node embedding in Equation 5 that does not consider
 340 the lead-lag relationship and multi-scale interaction effects. However, $\mathcal{V}^s \in \mathbb{R}^{(N \times T \times d)}$ is the spatio-
 341 temporal hypernode embedding in Equation 20 that incorporates lead-lag correlation and multi-
 342 scale information. Finally, we combine the prediction results at different scales to obtain the final
 343 prediction result.

345 3.7 OPTIMIZATION OBJECTIVES

347 Following StockMixer (Fan & Shen, 2024), we use the return ratio of a stock as the groundtruth.
 348 We use a combination of a pointwise regression and pairwise ranking-aware loss to minimize the
 349 MSE between the predicted and actual 1-day return ratios, while maintaining the relative order of
 350 top-ranked stocks with higher expected return for investment as follows.

$$351 \quad \mathcal{L}_{MSE} = \|\hat{Y} - Y\|_2^2, \quad \mathcal{L}_{Rank} = \sum_{i=1}^d \sum_{j=1}^d \max(0, -(\hat{r}_i^t - \hat{r}_j^t)(r_i^t - r_j^t)), \quad (23)$$

$$354 \quad \mathcal{L} = \mathcal{L}_{MSE} + \alpha \mathcal{L}_{Rank}, \quad (24)$$

355 where \hat{r}^t and r^t are the predicted and actual ranking scores, respectively, and α is a weight parameter.

357 4 EXPERIMENTS

359 4.1 EXPERIMENTAL SETUP

361 **Datasets.** We evaluate our approach using three real-world datasets from the US stock market.
 362 These datasets contain relatively complete stock-industry relationships or Wiki-based company re-
 363 lations. The NASDAQ and NYSE datasets (Feng et al., 2019b) include EOD data from 01/02/2013
 364 to 12/08/2017, filtered from the respective markets. Abnormal patterns and penny stocks were re-
 365 moved, while preserving their representative properties, with NASDAQ being more volatile and
 366 NYSE more stable. The S&P500 dataset (Huynh et al., 2023) gathers historical price data and in-
 367 dustry information for the companies listed in the S&P500 index from the Yahoo Finance database,
 368 covering the period from 01/04/2016 to 05/25/2022. The datasets statistics are provided in Table 4.

369 **Baselines.** We conduct a comparative analysis between our proposed Hermes and a range of base-
 370 line methods, which include prominent approaches in both machine learning and deep learning
 371 methods for STSF. Given that existing research has demonstrated the limited effectiveness of tradi-
 372 tional statistical methods (Fan & Shen, 2024; Li et al., 2024), we exclude them from our comparative
 373 evaluation to focus on more competitive approaches.

375 4.2 OVERALL PERFORMANCE

376 We present a detailed comparison of our approach (Hermes) with four types of baseline methods
 377 in Table 1. We have the following observations: 1) For univariate methods, whether it is LSTM or

378 Table 1: Comparison results on public stock market datasets (measured by t-test with p-value <
 379 0.01). The methods for comparison are mainly divided into four types: RNN (Recurrent Neural
 380 Network), GNN (Graph Neural Network), HGNN (HyperGraph Neural Network), and MLP (Multi-
 381 Layer Perceptron). Bold indicates the best (SOTA) results.

Model	NASDAQ				NYSE				S&P500				
	IC	RIC	prec@N	SR	IC	RIC	prec@N	SR	IC	RIC	prec@N	SR	
RNN	LSTM	0.032	0.354	0.514	0.892	0.024	0.256	0.512	0.857	0.031	0.186	0.531	1.332
	ALSTM	0.035	0.371	0.522	0.941	0.023	0.276	0.519	0.764	0.029	0.181	0.532	1.298
GNN	RGCN	0.034	0.382	0.516	1.054	0.025	0.275	0.517	0.932	0.028	0.175	0.528	1.359
	GAT	0.035	0.377	0.530	1.233	0.025	0.297	0.521	1.070	0.034	0.191	0.541	1.484
	RSR-I	0.038	0.398	0.531	1.238	0.026	0.284	0.519	0.998	0.033	0.200	0.542	1.437
MLP	Linear	0.019	0.188	0.505	0.517	0.015	0.163	0.497	0.625	0.016	0.156	0.520	0.674
	StockMixer	0.043	0.501	0.545	1.465	0.029	0.351	0.539	1.454	0.041	0.262	0.551	1.586
HGNN	STHAN-SR	0.039	0.451	0.543	1.416	0.029	0.344	0.542	1.228	0.037	0.227	0.549	1.533
	ESTIMATE	0.037	0.444	0.539	1.307	0.030	0.327	0.536	1.115	0.035	0.241	0.553	1.547
	Hermes (Ours)	0.044	0.538	0.535	2.161	0.032	0.466	0.549	1.655	0.050	0.334	0.539	2.247

394 ALSTM, their performance is inferior to that of other hybrid architectures. This strongly highlights
 395 the necessity and importance of capturing the complex industry and stock relationships in financial
 396 markets. 2) For GNNs algorithms such as RGCN, GAT, and RSR-I, their performance shows a
 397 significant improvement over RNNs, indicating that GNNs have strong stock relationship modeling
 398 capabilities. However, compared to HGNNs algorithms like STHAN-SR and ESTIMATE, GNNs
 399 perform slightly worse. This suggests that in the context of the financial market industry, using
 400 hypergraph models to unify the relationships of stocks within the industry plays a crucial role in
 401 enhancing forecasting performance. 3) The simple linear model fails due to insufficient inductive
 402 bias. While StockMixer strikes a balance between the simplicity of MLP models and the excellent
 403 performance of hybrid networks, it achieves the second-best results across most metrics. However,
 404 because MLP-based models inherently have smaller model capacities, the issue of insufficient inductive
 405 bias in StockMixer becomes more apparent when dealing with larger datasets. 4) Compared to
 406 other hypergraph algorithms that consider stock relationships within industries (such as STHAN-SR
 407 and ESTIMATE), the Hermes algorithm we propose shows significant performance improvement.
 408 This clearly demonstrates that, based on the consideration of stock relationships within industries,
 409 incorporating inter-industry lead-lag relationships and multi-scale relationships plays a crucial role
 410 in enhancing forecasting capability.

4.3 ABLATION STUDIES

413 Table 2 illustrates the unique impact of each module and contrasts them with two hypergraph-based
 414 baseline models, STHAN-SR and ESTIMATE. We have the following observations: 1) When the
 415 **multi-scale fusion module** in Section 3.5 and the **total multi-scale module** (Remove the Total
 416 Multi-Scale module, including Decomposition in Section 3.2 and Fusion in Section 3.5, respec-
 417 tively) are removed, the performance of the model decreases in both cases. The performance drop
 418 is more severe when the entire module is removed, indicating that while decomposition helps, the
 419 internal fusion of multi-scale information is key to further enhancing performance. 2) Ablating the
 420 lead-lag module in Section 3.4, which limits the model to only intra-industry correlations, causes
 421 a notable performance decline. This highlights the importance of modeling inter-industry lead-lag
 422 relationships. Even without this module, Hermes still outperforms STHAN-SR and ESTIMATE
 423 which only consider internal industry correlations, demonstrating the superiority of Hermes’s core
 424 architecture over other hypergraph-based approaches. 3) Removing the skip-connection module in
 425 Section 3.6 also reduces performance, confirming its crucial role in facilitating information trans-
 426 mission and gradient flow, thereby improving the model’s feature extraction capabilities.

4.4 EFFICIENCY ANALYSIS

430 In order to ensure good applicability of the model in practical applications, the runtime and memory
 431 usage of the model are crucial. We conducted an efficiency comparison analysis of Hermes and two
 432 other hypergraph-based methods, STHAN-SR and ESTIMATE—see Table 3.

432 Table 2: Ablation study results on public datasets NASDAQ, NYSE, and S&P500.
433

Ablation				NASDAQ				NYSE				S&P500				
Model Component	IC	ICIR	Prec@N	SR	IC	ICIR	Prec@N	SR	IC	ICIR	Prec@N	SR	IC	ICIR	Prec@N	SR
w/o Multi-Scale Fusion	0.038	0.464	0.521	1.374	0.028	0.421	0.545	1.354	0.031	0.248	0.531	1.517				
w/o Total Multi-Scale	0.030	0.422	0.506	0.975	0.023	0.347	0.527	1.199	0.032	0.213	0.503	1.075				
w/o Lead-Lag	0.039	0.472	0.526	1.451	0.028	0.420	0.540	0.225	0.037	0.201	0.519	1.628				
w/o Skip-Connection	0.041	0.441	0.536	1.655	0.029	0.345	0.539	1.449	0.043	0.252	0.522	1.653				
STHAN-SR	0.039	0.451	0.543	1.416	0.029	0.344	0.542	1.228	0.037	0.227	0.549	1.533				
ESTIMATE	0.037	0.444	0.539	1.307	0.030	0.327	0.536	1.115	0.035	0.241	0.553	1.547				
Hermes (Ours)	0.044	0.538	0.535	2.161	0.032	0.466	0.549	1.655	0.050	0.334	0.539	2.247				

441
442 Table 3: Efficiency analysis on public stock datasets, concerning the training time, inference time
443 (measured in milliseconds per batch under the condition of a batch size being 1), and memory usage
444 (quantified in GB) of different models.

Dataset			NASDAQ			NYSE			S&P500			
Property	STHAN-SR	ESTIMATE	Hermes	STHAN-SR	ESTIMATE	Hermes	STHAN-SR	ESTIMATE	Hermes	STHAN-SR	ESTIMATE	Hermes
Training Time	257 ms	1,267 ms	215 ms	384 ms	1,462 ms	282 ms	297 ms	1,317 ms	211 ms			
Inference Time	52 ms	163 ms	42 ms	73 ms	241 ms	61 ms	32 ms	109 ms	25 ms			
Memory Usage	2.15 GB	9.62 GB	0.98 GB	2.82 GB	10.25 GB	1.14 GB	1.23 GB	4.52 GB	0.54 GB			

451 **Runtime Analysis:** In practical application scenarios, fast response is one of the key factors. For
452 example, in the field of financial market forecasting, timely obtaining forecasting results can provide
453 valuable decision-making basis for investors. If the model takes too long to operate, even if the
454 prediction accuracy is high, it will be difficult to meet the actual needs. Therefore, we evaluate the
455 computational speed by recording the time each model takes to train and infer a sample (that is, the
456 batch size is uniformly set to 1) with the same dataset. The results show that the Hermes model
457 performs excellently. Compared with the other two hypergraph-based methods, its computational
458 time is reduced. This is mainly attributed to the fact that some modules of the Hermes model adopt
459 an efficient MLP structure in the algorithm design process. This structure can significantly improve
460 the computational efficiency while ensuring the accuracy of forecasting results.

461 **Memory Analysis:** Memory usage is also an important factor to measure the efficiency of the model.
462 Excessive memory usage will not only limit the application range of the model in different hardware
463 environments but also may cause the system to run slowly or even crash. In this experiment, we moni-
464 tored the memory usage of each model in detail during operation. The results show that the Hermes
465 has a lower memory usage rate. This advantage primarily stems from its unique architectural design,
466 which enables superior performance without requiring large hidden dimensions, as further validated
467 in Section B.5 through sensitivity analysis of the Latent Space Dimension parameter. Consequently,
468 Hermes effectively reduces memory usage while maintaining high performance, enhancing both the
469 practicality and deployment flexibility of the model.

470 5 CONCLUSIONS

471 Stock time series forecasting plays a pivotal role in the modern economy, serving as a key tool
472 for investors, financial institutions, and policymakers to make accurate decisions. However, existing
473 forecasting methods often fall short in fully considering the lead-lag between industries and
474 multi-scale information, resulting in limited predictive performance. To address these challenges,
475 this study introduces the Hermes framework. By ingeniously fusing multi-scale analysis with lead-
476 lag modules within a hypergraph network, the Hermes framework significantly boosts the per-
477 formance of stock forecasting. Specifically, the hyperedge-based moving aggregation module incor-
478 porates a sliding window and utilizes dynamic temporal aggregation operations to consider lead-lag
479 dependencies among industries. Meanwhile, the hyperedge-based multi-scale fusion module de-
480 composes raw data at multiple scales, and then employs cross-scale, edge-to-edge message pass-
481 ing to integrate information from different scales while preserving the consistency of each scale.
482 Experimental results on multiple real-world stock datasets show that Hermes outperforms exist-
483 ing state-of-the-art methods in both efficiency and accuracy. All datasets and code are available
484 at <https://anonymous.4open.science/r/Hermes-E150>.

486 ETHICS STATEMENT
487488 Our work exclusively uses publicly available benchmark datasets that contain no personally identi-
489 fiable information. No human subjects are involved in this research.
490491 REPRODUCIBILITY STATEMENT
492493 The promise that all experimental results can be reproduced. We have released our model code in
494 an anonymous repository: <https://anonymous.4open.science/r/Hermes-E150>.
495496 REFERENCES
497498 Md Shadman Abid, Razzaqul Ahshan, Mohammed Al-Abri, and Rashid Al Abri. Robust deep
499 learning model with attention framework for spatiotemporal forecasting of solar and wind energy
500 production. *Energy Conversion and Management: X*, pp. 100919, 2025.
501502 Ryo Akita, Akira Yoshihara, Takashi Matsubara, and Kuniaki Uehara. Deep learning for stock
503 prediction using numerical and textual information. In *ICIS*, pp. 1–6, 2016.
504505 Khalid Alkhatib, Hassan Najadat, Ismail Hmeidi, and Mohammed K Ali Shatnawi. Stock price
506 prediction using k-nearest neighbor (knn) algorithm. *IJBHT*, 3(3):32–44, 2013.
507508 Adebiyi Ariyo Ariyo, Aderemi Oluyinka Adewumi, and Charles K. Ayo. Stock price prediction
509 using the ARIMA model. In *ICCMS*, pp. 106–112, 2014.
510511 Chaofan Chen, Zelei Cheng, Zuoqian Li, and Manyi Wang. Hypergraph attention networks. In
512 *TrustCom*, pp. 1560–1565, 2020.
513514 Francis X Diebold and Kamil Yilmaz. On the network topology of variance decompositions: Mea-
515 suring the connectedness of financial firms. *Journal of econometrics*, 182(1):119–134, 2014.
516517 Edwin J Elton, Martin J Gruber, Stephen J Brown, and William N Goetzmann. *Modern portfolio*
518 *theory and investment analysis*. 2009.
519520 Christos Faloutsos, Jan Gasthaus, Tim Januschowski, and Yuyang Wang. Forecasting big time
521 series: old and new. In *Proc. VLDB Endow.*, pp. 2102–2105, 2018.
522523 Jinyong Fan and Yanyan Shen. Stockmixer: A simple yet strong mlp-based architecture for stock
524 price forecasting. In *AAAI*, pp. 8389–8397, 2024.
525526 Fuli Feng, Huimin Chen, Xiangnan He, Ji Ding, Maosong Sun, and Tat-Seng Chua. Enhancing
527 stock movement prediction with adversarial training. In *IJCAI*, pp. 5843–5849, 2019a.
528529 Fuli Feng, Xiangnan He, Xiang Wang, Cheng Luo, Yiqun Liu, and Tat-Seng Chua. Temporal
530 relational ranking for stock prediction. *TOIS*, 37(2):1–30, 2019b.
531532 Yifan Feng, Haoxuan You, Zizhao Zhang, Rongrong Ji, and Yue Gao. Hypergraph neural networks.
533 In *AAAI*, pp. 3558–3565, 2019c.
534535 Aditya Gupta and Bhuwan Dhingra. Stock market prediction using hidden markov models. In *SCES*,
536 pp. 1–4, 2012.
537538 Sepp Hochreiter and Jürgen Schmidhuber. Long short-term memory. *Neural computation*, 9(8):
539 1735–1780, 1997.
540541 Thanh Trung Huynh, Minh Hieu Nguyen, Thanh Tam Nguyen, Phi Le Nguyen, Matthias Weidlich,
542 Quoc Viet Hung Nguyen, and Karl Aberer. Efficient integration of multi-order dynamics and
543 internal dynamics in stock movement prediction. In *WSDM*, pp. 850–858, 2023.
544545 Kaippallimalil J Jacob and Dennis Shasha. Fintime: a financial time series benchmark. *ACM*
546 *SIGMOD Record*, 28(4):42–48, 1999.
547

540 Kyoung-jae Kim. Financial time series forecasting using support vector machines. *Neurocomputing*,
 541 55(1-2):307–319, 2003.

542

543 Diederik P. Kingma and Jimmy Ba. Adam: A method for stochastic optimization. In *ICLR*, 2015.

544

545 Ana Lazcano, Miguel A Jaramillo-Morán, and Julio E Sandubete. Back to basics: The power of the
 546 multilayer perceptron in financial time series forecasting. *Mathematics*, 12(12):1920, 2024.

547

548 Tong Li, Zhaoyang Liu, Yanyan Shen, Xue Wang, Haokun Chen, and Sen Huang. Master: Market-
 549 guided stock transformer for stock price forecasting. In *AAAI*, pp. 162–170, 2024.

550

551 Wei Li, Ruihan Bao, Keiko Harimoto, Deli Chen, Jingjing Xu, and Qi Su. Modeling the stock
 552 relation with graph network for overnight stock movement prediction. In *IJCAI*, pp. 4541–4547,
 2021.

553

554 Xiaojie Li, Chaoran Cui, Donglin Cao, Juan Du, and Chunyun Zhang. Hypergraph-based reinforce-
 555 ment learning for stock portfolio selection. In *ICASSP*, pp. 4028–4032, 2022.

556

557 Sihao Liao, Liang Xie, Yuanchuang Du, Shengshuang Chen, Hongyang Wan, and Haijiao Xu. Stock
 558 trend prediction based on dynamic hypergraph spatio-temporal network. *Applied Soft Computing*,
 154:111329, 2024.

559

560 Shengsheng Lin, Weiwei Lin, Wentai Wu, Haojun Chen, and Junjie Yang. Sparsesf: Modeling
 561 long-term time series forecasting with *1k* parameters. In *ICML*, pp. 30211–30226, 2024.

562

563 Shengsheng Lin, Weiwei Lin, Xinyi Hu, Wentai Wu, Ruichao Mo, and Haocheng Zhong. Cyclenet:
 564 enhancing time series forecasting through modeling periodic patterns. pp. 106315–106345, 2025.

565

566 Yongen Luo, Jicheng Hu, Xiaofeng Wei, Dongjian Fang, and Heng Shao. Stock trends prediction
 567 based on hypergraph modeling clustering algorithm. In *PIC*, pp. 27–31, 2014.

568

569 David MQ Nelson, Adriano CM Pereira, and Renato A De Oliveira. Stock market’s price movement
 570 prediction with lstm neural networks. In *IJCNN*, pp. 1419–1426, 2017.

571

572 Ashadun Nobi, Seong Eun Maeng, Gyeong Gyun Ha, and Jae Woo Lee. Effects of global financial
 573 crisis on network structure in a local stock market. *Physica A: Statistical Mechanics and its
 574 Applications*, 407:135–143, 2014.

575

576 FX Satriyo D Nugroho, Teguh Bharata Adj, and Silmi Fauziati. Decision support system for stock
 577 trading using multiple indicators decision tree. In *ICITACEE*, pp. 291–296, 2014.

578

579 Omowonuola Ireoluwapo Kehinde Olanrewaju, Gideon Oluseyi Daramola, and Darlington Eze
 580 Ekechukwu. Strategic financial decision-making in sustainable energy investments: Leverag-
 581 ing big data for maximum impact. *World Journal of Advanced Research and Reviews*, 22(3):
 582 564–573, 2024.

583

584 Adam Paszke, Sam Gross, Francisco Massa, Adam Lerer, James Bradbury, Gregory Chanan, Trevor
 585 Killeen, Zeming Lin, Natalia Gimelshein, Luca Antiga, Alban Desmaison, Andreas Köpf, Ed-
 586 ward Z. Yang, Zachary DeVito, Martin Raison, Alykhan Tejani, Sasank Chilamkurthy, Benoit
 587 Steiner, Lu Fang, Junjie Bai, and Soumith Chintala. Pytorch: An imperative style, high-
 588 performance deep learning library. In *NeurIPS*, pp. 8024–8035, 2019.

589

590 Yao Qin, Dongjin Song, Haifeng Chen, Wei Cheng, Guofei Jiang, and Garrison Cottrell. A
 591 dual-stage attention-based recurrent neural network for time series prediction. *arXiv preprint
 592 arXiv:1704.02971*, 2017.

593

594 Xiangfei Qiu, Jilin Hu, Lekui Zhou, Xingjian Wu, Junyang Du, Buang Zhang, Chenjuan Guo, Aoy-
 595 ing Zhou, Christian S. Jensen, Zhenli Sheng, and Bin Yang. Tfb: Towards comprehensive and fair
 596 benchmarking of time series forecasting methods. In *Proc. VLDB Endow.*, pp. 2363–2377, 2024.

597

598 Xiangfei Qiu, Xiuwen Li, Ruiyang Pang, Zhicheng Pan, Xingjian Wu, Liu Yang, Jilin Hu, Yang
 599 Shu, Xuesong Lu, Chengcheng Yang, Chenjuan Guo, Aoying Zhou, Christian S. Jensen, and Bin
 600 Yang. Easyme: Time series forecasting made easy. In *ICDE*, 2025.

594 S Saba Rafiei, Mahdi S Naderi, and Mehrdad Abedi. A comprehensive energy management applica-
 595 tion method considering smart home occupant behavior using iot and real big data. *arXiv preprint*
 596 *arXiv:2502.06052*, 2025.

597

598 Mohammad Obaidur Rahman, Md Sabir Hossain, Ta-Seen Junaid, Md Shafiu1 Alam Forhad, and
 599 Muhammad Kamal Hossen. Predicting prices of stock market using gated recurrent units (grus)
 600 neural networks. *International Journal of Computer Science and Network Security*, 19(1):213–
 601 222, 2019.

602 Akhter Mohiuddin Rather, VN Sastry, and Arun Agarwal. Stock market prediction and portfolio
 603 selection models: a survey. *Opsearch*, 54:558–579, 2017.

604

605 Ramit Sawhney, Shivam Agarwal, Arnav Wadhwa, and Rajiv Ratn Shah. Spatiotemporal hypergraph
 606 convolution network for stock movement forecasting. In *ICDM*, pp. 482–491, 2020.

607

608 Ramit Sawhney, Shivam Agarwal, Arnav Wadhwa, Tyler Derr, and Rajiv Ratn Shah. Stock selection
 609 via spatiotemporal hypergraph attention network: A learning to rank approach. In *AAAI*, pp. 497–
 610 504, 2021.

611 William F Sharpe. The sharpe ratio. *Journal of portfolio management*, 21(1):49–58, 1994.

612 Arash Tashakkori, Mohammad Talebzadeh, Fatemeh Salboukh, and Lochan Deshmukh. Forecasting
 613 gold prices with mlp neural networks: A machine learning approach. *IJSEA*, pp. 13–20, 2024.

614

615 Petar Veličković, Guillem Cucurull, Arantxa Casanova, Adriana Romero, Pietro Lio, and Yoshua
 616 Bengio. Graph attention networks. *arXiv preprint arXiv:1710.10903*, 2017.

617

618 Sheng Xiang, Dawei Cheng, Chencheng Shang, Ying Zhang, and Yuqi Liang. Temporal and het-
 619 erogeneous graph neural network for financial time series prediction. In *CIKM*, pp. 3584–3593,
 620 2022.

621

622 Furong Ye, Liming Zhang, Defu Zhang, Hamido Fujita, and Zhiguo Gong. A novel forecasting
 623 method based on multi-order fuzzy time series and technical analysis. *Information Sciences*, 367:
 41–57, 2016.

624

625 Ailing Zeng, Muxi Chen, Lei Zhang, and Qiang Xu. Are transformers effective for time series
 626 forecasting? In *AAAI*, pp. 11121–11128, 2023.

627

628 Rui Zhang, Reshu Jain, Prasenjit Sarkar, and Lukas Rupprecht. Getting your big data priorities
 629 straight: a demonstration of priority-based qos using social-network-driven stock recommenda-
 630 tion. In *Proc. VLDB Endow.*, pp. 1665–1668, 2014.

631

632 Zetao Zheng, Jie Shao, Jia Zhu, and Heng Tao Shen. Relational temporal graph convolutional
 633 networks for ranking-based stock prediction. In *ICDE*, pp. 123–136, 2023.

634

635

636

637

638

639

640

641

642

643

644

645

646

647

648 **A APPENDIX**
649650 **A.1 THE USE OF LARGE LANGUAGE MODELS (LLMs)**
651652 We do not use Large Language Models in our methodology and writing.
653654 **A.2 EXPERIMENTAL SETUP**
655656 **A.2.1 DATASETS**
657658 To validate the performance of Hermes, we use three publicly available stock market datasets,
659 with the dataset statistics provided in Table 4. These datasets provide a diverse set of stock time
660 series, allowing us to comprehensively assess the model’s effectiveness across different financial
661 scenarios. We evaluate our approach using three real-world datasets from the US stock market.
662 These datasets contain relatively complete stock-industry relationships or Wiki-based company re-
663 lations. The NASDAQ and NYSE datasets (Feng et al., 2019b) include EOD data from 01/02/2013
664 to 12/08/2017, filtered from the respective markets. Abnormal patterns and penny stocks were re-
665 moved, while preserving their representative properties, with NASDAQ being more volatile and
666 NYSE more stable. The S&P500 dataset (Huynh et al., 2023) gathers historical price data and in-
667 dustry information for the companies listed in the S&P500 index from the Yahoo Finance database,
668 covering the period from 01/04/2016 to 05/25/2022.
669670 **Table 4: Statistics of datasets.**
671672

Property	Dataset	NASDAQ	NYSE	S&P500
# Stocks	1026	1737	474	
# Industries	113	130	11	
# Technical Indicators	5	5	5	
Start Time	13-01-02	13-01-02	16-01-04	
End Time	17-12-08	17-12-08	22-05-25	
Total Time Steps	1281	1281	1611	
Train Time Steps	756	756	1006	
Validate Time Steps	252	252	253	
Test Time Steps	273	273	352	

686 **A.2.2 IMPLEMENTATION DETAILS**
687688 For fair comparison, all samples are generated by moving a 16 time steps lookback window. All
689 experiments with Hermes are conducted using PyTorch (Paszke et al., 2019) in Python 3.9, and are
690 executed on a server featuring an Intel(R) Xeon(R) Platinum 8358 CPU and an NVIDIA Tesla-A800
691 GPU. We use ADAM (Kingma & Ba, 2015) with an initial learning rate of 5e - 3. The “*Drop Last*”
692 issue is reported by several researchers (Qiu et al., 2024; 2025). That is, in some previous works
693 evaluating the model on test set with drop-last=True setting may cause additional errors related to
694 test batch size. In our experiment, to ensure fair comparison in the future, we set the drop last to
695 False for all baselines to avoid this issue.
696697 **A.2.3 METRICS**
698699 Previous studies use different evaluation metrics, making it challenging to perform a comprehensive
700 comparison of various methods. To provide a thorough assessment of the methods performance, we
701 use four of the most commonly applied and reliable metrics: **IC** and **ICIR**, which are rank-based
evaluation metrics; **Prec@N**, which measures accuracy; and **SR**, which is return-based.

702 • **Information Coefficient (IC):** IC is a coefficient that shows how close the prediction is to the
 703 actual result, computed by the average pearson correlation coefficient.
 704

$$705 \quad IC_t = \frac{1}{N} \frac{(\hat{Y}_t - \text{mean}(\hat{Y}_t))^T (Y_t - \text{mean}(Y_t))}{\text{std}(\hat{Y}_t) \cdot \text{std}(Y_t)}, \quad (25)$$

706 where Y_t are the raw stock price trends and \hat{Y}_t are the model predictions at each timestamp. We
 707 report the average IC over all test dataset.
 708

709 • **Information Ratio-based Information Coefficient (ICIR):** The information ratio of the IC met-
 710 ric, calculated by:
 711

$$712 \quad ICIR = \frac{\text{mean}(IC)}{\text{std}(IC)}. \quad (26)$$

713 • **Precision@N (Prec@N):** Prec@N evaluates the precision of the top N short-term profit pre-
 714 dictions from the model. This way, we assess the capability of the techniques to support investment
 715 decisions. For example, when N is 10, and the labels of 6 among these top 10 predictions are
 716 positive, then the Prec@10 is 60%.
 717

$$718 \quad Prec@N = \frac{TP@N}{N}, \quad (27)$$

719 where TP is the number of true positive classifications. In this study, N is set to 10.
 720

721 • **Sharpe Ratio (SR):** Sharpe ratio (Sharpe, 1994) measures the profitability of the investment
 722 method and take into account risk.
 723

$$724 \quad SR = \frac{E_t[\rho_t - \rho_F]}{\sqrt{\text{var}_t(\rho_t - \rho_F)}}, \quad (28)$$

725 where $\rho_t = \frac{p_t}{p_{t-1}} - 1$ is the return on the portfolio and p_F is the return on the risk-free asset which
 726 is always 0.
 727

728 A.2.4 BASELINES

729 We conduct a comparative analysis between our proposed Hermes and a range of baseline meth-
 730 ods, which include prominent approaches in both machine learning and deep learning methods for
 731 STSF. Given that existing research has demonstrated the limited effectiveness of traditional statisti-
 732 cal methods (Fan & Shen, 2024; Li et al., 2024), we exclude them from our comparative evaluation
 733 to focus on more competitive approaches.
 734

735 • **LSTM** (Hochreiter & Schmidhuber, 1997) refers to the standard LSTM model, which operates
 736 on sequential data, including closing prices and moving averages over 5, 10, 20, and 30 days, to
 737 generate a sequential embedding. A fully connected (FC) layer is then employed to predict the
 738 return ratio.
 739 • **ALSTM** (Feng et al., 2019a) integrates adversarial training and stochastic simulation into an
 740 enhanced LSTM model, allowing it to more effectively capture market dynamics.
 741 • **RGCN** (Li et al., 2021) introduces a model that captures both positive and negative correlations
 742 among stocks using a correlation matrix computed from historical market data. The LSTM mech-
 743 anism in RGCN layers helps mitigate over-smoothing issues when predicting overnight stock
 744 price movements.
 745 • **GAT** (Veličković et al., 2017) employs Graph Attention Networks (GAT) to aggregate stock
 746 embeddings, which are encoded by a GRU, on the stock graph. By combining the advantages of
 747 Graph Neural Networks (GNN) and attention mechanisms, it enhances performance in large-scale
 748 graph settings.
 749 • **RSR** (Feng et al., 2019b) introduces a novel neural network-based framework called Relational
 750 Stock Ranking, which addresses the stock forecasting problem in a learning-to-rank approach.
 751 Additionally, it proposes a new component in neural network modeling, called Temporal Graph
 752 Convolution, which is designed to explicitly capture the domain knowledge of stock relationships
 753 in a time-sensitive manner.
 754

- 756 • **STHAN-SR** (Sawhney et al., 2021) introduces a novel Spatio-Temporal Hypergraph Attention
757 Network that models inter-stock relationships of different types and strengths as a hypergraph
758 for stock ranking. It combines temporal Hawkes attention with spatial hypergraph convolutions
759 through hypergraph attention to capture both the correlations in the movements of related stocks
760 and the temporal evolution of their historical features.
- 761 • **ESTIMATE** (Huynh et al., 2023) integrates temporal generative filters within a memory-based
762 shared parameter LSTM network, enhancing the model’s ability to learn temporal patterns for
763 each stock. Furthermore, it introduces attention hypergraph convolutional layers that utilize the
764 wavelet basis—a convolution approach that leverages the polynomial wavelet basis to streamline
765 message passing and focus on localized convolutions.
- 766 • **Linear** (Zeng et al., 2023) employs a straightforward approach by utilizing only fully connected
767 layers to predict the final price. This method does not incorporate any advanced architectures or
768 temporal dependencies, relying solely on basic linear transformations to generate the forecasting.
769 Despite its simplicity, it serves as a baseline model for comparison with more complex models.
- 770 • **StockMixer** (Fan & Shen, 2024) introduces a lightweight yet effective MLP-based architecture
771 for stock price forecasting. The model incorporates three key components—indicator mixing,
772 time mixing, and stock mixing—which work together to capture the intricate correlations within
773 the stock data.

774 B RELATED WORK

775 B.1 TRADITIONAL STOCK TIME SERIES FORECASTING

776 Early stock forecasting methods rely mainly on statistical learning techniques to capture patterns
777 and relationships in time series (Ye et al., 2016; Ariyo et al., 2014; Gupta & Dhingra, 2012; Elton
778 et al., 2009). One of the most widely used techniques is the Autoregressive Integrated Moving
779 Average (ARIMA) (Ariyo et al., 2014) model, which stabilizes data by combining Autoregressive
780 components, Moving Average, and differencing, thereby modeling time series. Another commonly
781 used traditional method is the Hidden Markov Model (HMM) (Gupta & Dhingra, 2012), which is
782 used to describe unobservable states in the market and can detect changes in market conditions,
783 making it suitable for analyzing market transitions. Although these methods provide predictive
784 capabilities, they exhibit significant limitations when dealing with nonlinear, dynamic changes, and
785 sudden events in financial markets. As a market environment becomes more complex, traditional
786 statistical methods increasingly fail to provide sufficient predictive accuracy and robustness.

787 With the rapid development in machine learning, machine learning methods for stock time series
788 forecasting have emerged (Alkhatib et al., 2013; Nugroho et al., 2014; Kim, 2003). For example,
789 Support Vector Machines (SVMs) (Kim, 2003) map data to high-dimensional spaces using kernel
790 functions and find optimal separating hyperplanes in those spaces, which allows them to capture
791 complex relationships and dynamics in financial markets. However, SVMs are highly sensitive
792 to parameter selection and often struggles to capture long-term dependencies. Overall, although
793 machine learning methods show considerable potential in stock forecasting, they still rely on manual
794 feature engineering and model design. Moreover, these traditional stock forecasting methods have
795 not delved into the exploration of lead-lag relationships and multi-scale modeling.

796 B.2 DEEP LEARNING STOCK TIME SERIES FORECASTING

797 With the rise of deep learning, notable progress has occurred in stock forecasting. This is mainly
798 because deep neural networks can model complex nonlinear patterns. This is mainly because deep
799 neural networks can model complex nonlinear patterns. Some studies use recurrent neural networks
800 (RNNs) (Nelson et al., 2017; Qin et al., 2017; Akita et al., 2016; Rahman et al., 2019) to capture the
801 historical development in individual stock prices and predict their short-term trends. For example,
802 Long Short-Term Memory (LSTM) networks combined with historical stock data and text information
803 are used to predict stock prices (Akita et al., 2016). In addition, due to the significant progress
804 of Multi-Layer Perceptrons (MLPs) architecture in the general time series field, the DLinear (Zeng
805 et al., 2023), CycleNet (Lin et al., 2025), and SparseTSF (Lin et al., 2024) show the benefits of this
806 simple architecture for time series forecasting. Increasingly may proposals target stock forecasting
807 performance by improving the MLPs architecture. For example, a series of studies (Fan & Shen,
808

2024; Lazcano et al., 2024; Tashakkori et al., 2024) enhance the learning ability of simple MLPs structures by utilizing the MLP-Mixer backbone, thereby improving forecasting accuracy. Next, the Transformer model has become increasingly popular due to the ability of its self-attention mechanism to capture long-term dependencies. For example, Master (Li et al., 2024) proposes a novel stock transformer for stock price forecasting to effectively capture stock correlation.

Some deep learning models have begun to explore lead-lag relationships and multi-scale modeling. For instance, StockMixer (Fan & Shen, 2024) engages in multi-scale modeling by segmenting the original time series into subsequence-level patches and mixing features at different scales. However, this approach lacks effective integration of information across scales; it merely concatenates information from different scales without thorough fusion. On the other hand, ESTIMATE (Huynh et al., 2023) takes into account lead-lag relationships through data-driven detection of leading and lagging time series clusters. Nonetheless, this method falls short in capturing fine-grained lead-lag dynamics, as clustering can only reveal global lead-lag relationships. Distinctive from the aforementioned approaches, Hermes employs a sliding window technique and utilizes dynamic temporal aggregation operations to consider fine-grained lead-lag dependencies among stock industries. Moreover, it features a multi-scale fusion module, which utilizes a cross-scale, egde-to-edge message-passing to integrate information from different scales while maintaining the consistency of each scale.

While these deep learning methods have advanced stock forecasting, the complexity of stock data and the need to account for intricate relationships among stocks have led researchers to explore new methods based on hypergraphs.

B.3 HYPERGRAPH-BASED STOCK TIME SERIES FORECASTING

Traditional graphs have limitations when it comes to modeling higher-order multivariate relationships, as they can only represent relations between pairs of nodes. To address this issue, Hypergraph Neural Networks (HGNNS) (Feng et al., 2019c) were introduced. Hypergraphs extend the concept of simple graphs to enable the capture of relationships among multiple stocks (Chen et al., 2020). Hypergraphs have gained increasing attention and application across various fields. Hyperedge in a hypergraph represents a set of vertices, making them suitable for modeling non-pairwise relationships (Luo et al., 2014; Sawhney et al., 2020). For example, HGAM (Li et al., 2022) is a hypergraph-based reinforcement learning method for stock portfolio selection. THGNN (Xiang et al., 2022) is a temporal and heterogeneous graph neural network model that aims to learn dynamic relationships by using two-stage attention mechanisms. STHAN-SR (Sawhney et al., 2021) enhances corporate relevance based on Wiki data and uses hypergraph convolution to propagate information from higher-order neighbors. DHSTN (Liao et al., 2024) is a dynamic hypergraph network for learning spatio-temporal relations of stocks. Dynamic hypergraphs are generated adaptively using (Graph Attention Networks) GATs to capture time-varying higher-order spatial relationships among stocks. The latest method, ESTIMATE (Huynh et al., 2023), employs hypergraphs to capture non-pairwise correlations, utilizing temporal generative filters to identify individual patterns for each stock.

Unlike the above methods, we propose a new hypergraph-based stock forecasting model that specifically takes into account the multi-scale nature of stock data, enabling it to capture the complexity of market dynamics more comprehensively. Furthermore, our approach places particular emphasis on the lead-lag relationships between financial industries, where the changes in one industry may precede or lag behind those in another. By capturing these key relationships more fully, we aim to improve forecasting accuracy.

B.4 ILLUSTRATION FIGURES

B.5 HYPERPARAMETER SENSITIVITY

This experiment addresses question RQ3 on the hyperparameter sensitivity. Due to space limitations, we focus on the most important hyperparameters—see Figure 5.

Lookback window length T : We examine the predictive performance of Hermes as we adjust the lookback window length, T , illustrated in Figure 5a. Consistently across all datasets, a balanced window length emerges as the most effective. Window lengths that are too short result in a swift decline in performance due to inadequate information, whereas excessively lengthy sequences also

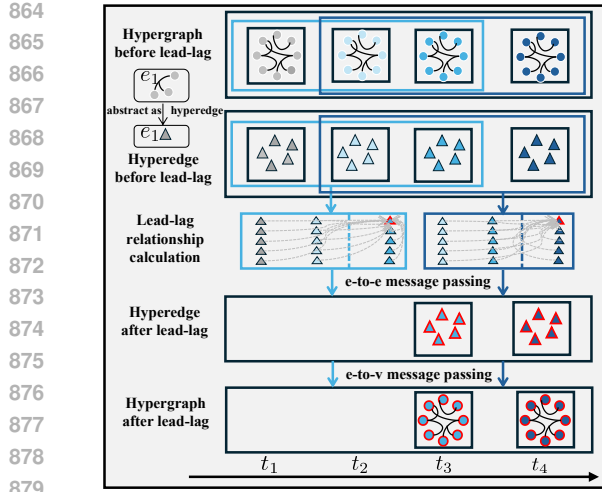


Figure 3: The specific lead-lag interaction process within the window, with a lead-lag step of 3 as an example.

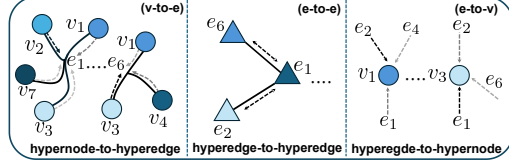


Figure 4: Three types of message passing: hypernodes for stocks and hyperedges for industries.

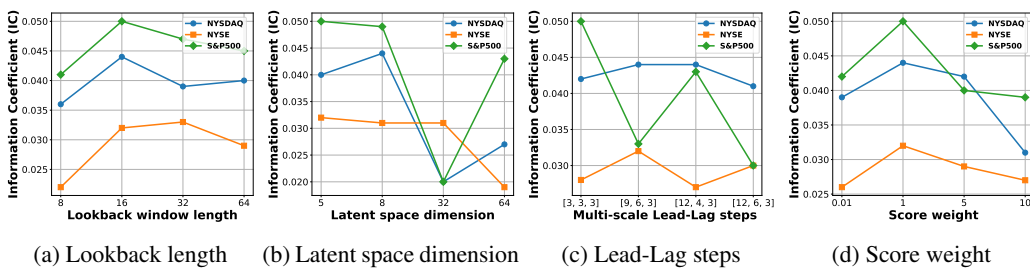


Figure 5: Parameter sensitivity studies of main hyper-parameters in Hermes.

underperform because of the absence of timely information benefits and the heightened learning expenses for stocks.

Latent space dimension d : In Section 3.2, we enhance the representational capacity of indicators by mapping them into a high-dimensional hidden space d , thereby facilitating the extraction of more intricate hidden relationships. In Figure 5b, we explore the impact of different hidden dimensions d and observe that datasets exhibit optimal performance at varying m values. Notably, when d is set to smaller values such as 5 or 8, models tend to achieve good performance; however, as d increases, models become prone to overfitting, leading to a decline in performance. Furthermore, selecting smaller d not only improves model performance but also effectively reduces the number of model parameters.

Multi-scale Lead-Lag steps w^1, w^2, \dots, w^S : In Section 3.4, for time series at each scale, we study the lead-lag correlations within w^s time steps to better extract complex dependencies in the time series, thereby improving forecasting performance. Here, we select three scales and specify the lead-lag time steps as w^1, w^2 , and w^3 , respectively. As shown in Figure 5c, we find that different datasets have variations in their multi-scale lead-lag time steps when achieving optimal performance. This is because different datasets possess unique characteristics, and their cyclicity (fine-grained scale) and trend (coarse-grained scale) may change due to external factors. Therefore, we recommend adjusting this parameter specifically when dealing with new datasets.

Score weight α : Besides, we adopt the score weight in section 3.7 to trade off the MSE loss and the ranking-aware loss—see Figure 5d. Experimental results show that all datasets achieve optimal performance and exhibit high stability when the score weight is set to 1. Therefore, we recommend setting this parameter to 1 in future research to obtain more optimized results.